Passive Vibration Control of the SCOLE Beam System

Xin Tong and Xiaowei Zhao*

Abstract

We investigate the optimization of multiple tuned mass dampers (TMDs) to reduce vibrations of flexible structures described by partial differential equations, using the non-uniform SCOLE (NASA Spacecraft Control Laboratory Experiment) beam system with multiple dominant modes as an illustrative application. We use multiple groups of TMDs with each group being placed at the antinode of the mode shape of a dominant mode of the SCOLE beam. We consider both the harmonic and random excitations, for which we employ frequency-limited $\mathcal{H}_\infty$ and $\mathcal{H}_2$ optimizations respectively to determine the parameters of the TMDs. Our optimization scheme takes into account the trade-off between effectiveness and robustness of the multiple TMDs to suppress the multiple dominant modes of the SCOLE beam. Simulation studies show that our scheme achieves substantial improvements over the traditional methods in terms of both effectiveness and robustness and that with equal total mass, TMD systems with each group having multiple TMDs are more effective and more robust than the ones with each group having a single TMD.

Index Terms

Flexible structures, partial differential equations, multiple tuned mass dampers, vibration suppression, finite element method, $\mathcal{H}_\infty/\mathcal{H}_2$ optimization.

I. Introduction

THE tuned mass damper (TMD) is a simple but widely-used passive structural control device comprising a mass, springs and dampers. The mass is linked to the main structure to be stabilized via springs and dampers. It has been successfully devised in building structures to reduce vibrations due to environmental excitations such as strong winds and earthquakes. For example the John Hancock Tower in Boston and the Citicorp Center in Manhattan have employed TMD systems to combat the wind's effects [1], whose mass components are put on the high floor of the building through wheels, see Fig. 1. These TMDs reduce about 50% of worst-case wind-induced motions. The Taipei 101 skyscraper contains the world's largest and heaviest TMD whose mass component is hung above the floor through cables [2]. This TMD reduces up to 40% of the tower's motion caused by strong winds.

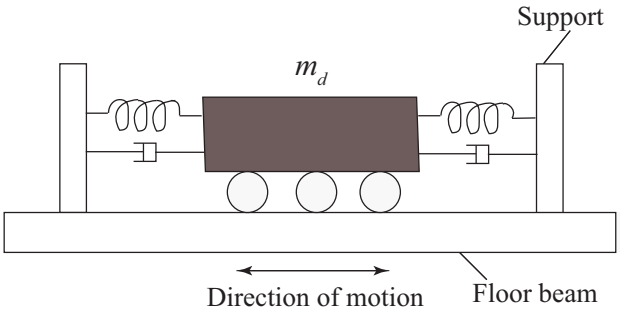

Fig. 1. Schematic diagram of the TMD systems used in the John Hancock Tower in Boston and the Citicorp Center in Manhattan, taken from the literature [3].

X.Tong and X. Zhao* are with the School of Engineering, University of Warwick, Coventry, CV4 7AL, United Kingdom, e-mail: xin.tong@warwick.ac.uk; xiaowei.zhao@warwick.ac.uk. *Corresponding author. Tel.: +44 (0)24 765 23145. Fax: +44 (0)24 76 418922.

In terms of the design of a single TMD, Den Hartog derived formulae for the optimal parameters of a TMD system to suppress harmonic excitations [4] while other researchers [5]–[7] provided formulae for the case of random excitations. In addition, Younesian et al. [8] proposed a TMD optimization scheme through minimizing the root mean square (RMS) of system displacements to suppress vibrations of Timoshenko beams subject to random excitations with peaked power spectral densities (PSDs). Furthermore, Leung et al. [9] applied the particle swarm optimization algorithm to optimize TMD parameters for the structure under non-stationary excitations. All these studies deal with the case of suppressing a single dominant vibration mode of the main structure using a single TMD. Dominant modes means the modes which contribute significantly to the vibrations.

For main structures with one dominant vibration mode, multiple TMDs with natural frequencies distributed around the dominant frequency are more effective and more robust than a single TMD with equal total mass [10]–[13]. Robustness of the TMD system is usually tested by mistuning, where modal frequencies of the main structure deviate from corresponding frequency utilized in the design of the TMDs [13]. Mistuning may be caused by estimation errors of modal frequencies of the main structure, changes of modal frequencies due to external loading, and/or manufacturing errors of TMDs [14], [15]. For main structures with several dominant vibration modes that all respond to seismic loads, Clark [16] designed multiple TMDs in such a way that each TMD was tuned for a dominant mode, based on Den Hartog's formulae [4]. Bergman et al. [17] placed TMDs on several floors of a building. The TMD tuned for the first mode played the most part in damping vibrations of the building while other dampers tuned for higher modes further improved the damping performances. Lewandowski and Grzymisawska [18] employed multiple TMDs with each TMD tuned for a selected vibration mode to reduce vibrations of a building, using Warburton's formulae [7]. Moon [19] used multiple TMDs vertically distributed along a building to control its first and higher vibration modes to resist winds. Fu and Johnson [20] utilized shading fins of a building as mass dampers to reduce earthquake-induced vibrations, demonstrating that the proposed near-optimal mass damper system performed better than a single TMD system through simulation studies.

In this paper, we study the vibration reduction of the non-uniform SCOLE (NASA Spacecraft Control Laboratory Experiment) model [21] subject to harmonic and random excitations using multiple TMDs based on $\mathcal{H}_\infty$ and $\mathcal{H}_2$ optimizations, respectively. Originally developed to model an uniform mast bearing an antenna located on a satellite [22], [23], the SCOLE system has become a widely-used model for a flexible beam with one end fixed and the other end linked to a rigid body. The SCOLE beam system was used to model a monopile wind turbine tower in either the side-side plane or the fore-aft plane [24], [25]. In our paper [25], we incorporated a single TMD into the nacelle on top of this wind turbine tower model in each of the side-side and fore-aft planes. Then we spatially discretized this tower-TMD model using spectral element method and derived the optimal parameters of the TMD system using $\mathcal{H}_2$ optimization. Simulation studies based on the NREL (National Renewable Energy Laboratory) 5-MW monopile wind turbine model [26] within FAST (Fatigue, Aerodynamics, Structures, and Turbulence) simulation environment [27] showed that this TMD system achieved substantial vibration reduction subject to random wind and wave loading. Because a typical monopile wind turbine tower only has one dominant mode in each of the side-side and fore-aft planes, a single TMD can work well if the dominant modal frequency remains fixed. This paper is an extension of our paper [25] to suppress multiple vibration modes of a general SCOLE beam using multiple TMDs and to increase the system robustness against mistuning effects, under harmonic and random excitations. We mention that either the $\mathcal{H}_\infty$ optimization or the $\mathcal{H}_2$ optimization can handle both types of excitations. But $\mathcal{H}_\infty$ optimization can get better suppression performance for harmonic excitations than $\mathcal{H}_2$ optimization while $\mathcal{H}_2$ optimization can get better suppression performance for random excitations than $\mathcal{H}_\infty$ optimization. So in practice the optimization method should be chosen based on the spectra of excitation signals.

The structure of the paper is as follows. In Section II, we first incorporate multiple TMDs into the non-uniform SCOLE model. Then we spatially discretize the infinite-dimensional SCOLE-TMD system Σ into a finite-dimensional model Σ_d using the finite element method (FEM). In Section III, we propose

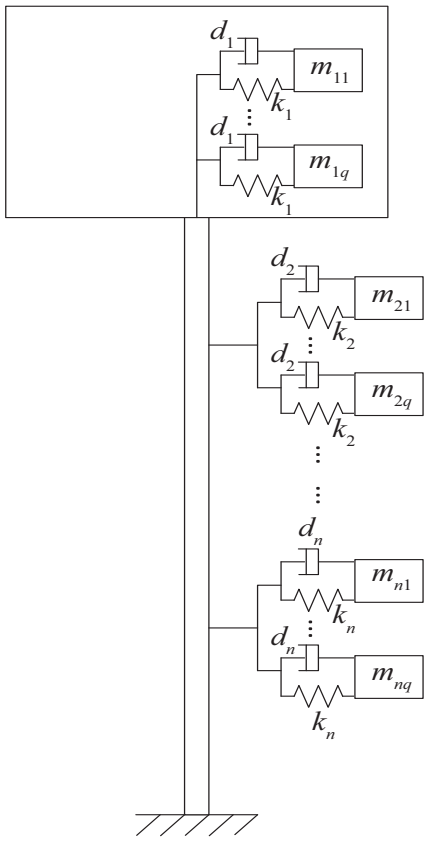

Fig. 2. A SCOLE beam system stabilized by multiple groups of TMDs.

a scheme for the optimization of the parameters of the multiple TMDs in Σ_d based on the $\mathcal{H}_\infty$ and $\mathcal{H}_2$ optimizations to suppress vibrations of the non-uniform SCOLE model with several dominant modes under harmonic and random excitations, respectively. Finally in Section IV, we examine performances of different TMD systems designed by our scheme and compare our scheme against traditional methods.

II. System Modelling

In this section, we design multiple groups of TMDs to reduce vibrations of the non-uniform SCOLE model which has multiple dominant vibration modes. The number of TMD groups is equal to the number of dominant vibration modes of the SCOLE model. Each group of TMDs is used to control a dominant mode of the SCOLE model, placed at the antinode of the corresponding mode shape [16], [19], [28], [29]. So the TMD groups are distributed along the beam, as in Fig. 2. Each TMD group contains the same number of TMDs. The TMDs in each TMD group have equal spring and damping constants but different masses with natural frequencies uniformly distributed around a central frequency which is close to the frequency of the corresponding mode to be controlled [10]. If the mode shape of a dominant mode has several antinodes, the corresponding TMD group is divided into sub-groups whose number is the same as the antinode number [30]. Other design procedures for this TMD group remain the same. For the sake of simplicity (but without loss of generality), the mode shape of each dominant mode of the SCOLE beam has a single antinode here.

For a non-uniform SCOLE model with n dominant vibration modes controlled by n groups of TMDs as shown in Fig. 2 (assuming that the antinode of the mode shape of the first dominant mode is at the

beam top), properties of the ith ($i = 1, 2, \cdots, n$) TMD group tuned to suppress the ith mode are

$$\omega_{ij} = \omega_T^i \left[1 + \left(j - \tfrac{q+1}{2}\right) \tfrac{B_W^i}{q-1}\right], \tag{2.1}$$

$$k_i = m_T^i \left(\textstyle\sum_{j=1}^{q} \frac{1}{\omega_{ij}^2}\right)^{-1}, \tag{2.2}$$

$$d_i = 2\zeta_i k_i (\omega_T^i)^{-1}, \tag{2.3}$$

$$m_{ij} = \tfrac{k_i}{\omega_{ij}^2}, \tag{2.4}$$

where ω_{ij} and m_{ij} are the natural frequency and the mass of the jth ($j = 1, 2, \cdots, q$) TMD in the ith TMD group, respectively. k_i and d_i are the spring and damping constants of all the TMDs in the ith TMD group. q is the number of TMDs in each TMD group, so the number of TMDs is $N_T = nq$. One can choose a practical value for q according to actual situation. ω_T^i, B_W^i, $m_T^i (= \sum_{j=1}^{q} m_{ij})$, ζ_i are the central frequency, the non-dimensional frequency bandwidth (w.r.t ω_T^i), the total mass, and the average damping ratio of the ith TMD group respectively, which are design variables to be optimized. A special case is that if $q = 1$ then $B_W^i = 0$.

The mathematical model Σ of the non-uniform SCOLE model coupled with n TMD groups with each group having q TMDs located at the antinode of the mode shape of a dominant mode as shown in Fig. 2 is given below:

$$\begin{cases}
\rho(x) w_{tt}(x,t) + (EI(x) w_{xx}(x,t))_{xx} = f_1, & (2.5)\\
(x,t) \in (0,l) \times [0,\infty), & \\
f_1 = \displaystyle\sum_{i=2}^{n} \delta(x - x_T^i) \sum_{j=1}^{q} \{k_i [p^{ij}(t) - w(x_T^i, t)] & \\
\qquad + d_i [p_t^{ij}(t) - w_t(x_T^i, t)]\}, & (2.6)\\
w(0,t) = 0,\ w_x(0,t) = 0, & (2.7)\\
m w_{tt}(l,t) - (EI w_{xx})_x(l,t) = F_e(t) + f_2, & (2.8)\\
f_2 = \displaystyle\sum_{j=1}^{q} \{k_1 [p^{1j}(t) - w(l,t)] & \\
\qquad + d_1 [p_t^{1j}(t) - w_t(l,t)]\}, & (2.9)\\
J w_{xtt}(l,t) + EI(l) w_{xx}(l,t) = T_e(t), & (2.10)\\
m_{ij} p_{tt}^{ij}(t) = -k_i [p^{ij}(t) - w(x_T^i, t)] & \\
\qquad\qquad - d_i [p_t^{ij}(t) - w_t(x_T^i, t)], & (2.11)
\end{cases}$$

where the subscripts t and x denote derivatives with respect to the time t and the position x. The equations (2.5)-(2.10) are the non-uniform SCOLE subsystem while the equation (2.11) describes the dynamics of each TMD of the TMD subsystem. l, ρ and EI denote the beam's height, the mass density function and the flexural rigidity function while w denotes the translational displacement of the beam. ρ and EI are assumed to be strictly positive functions. The parameters $m < 0$ and $J > 0$ are the mass and the moment of inertia of the rigid body. F_e and T_e denote the external force and torque excitations acting on the rigid body. $p^{ij}(t)$ ($i = 1, 2, \cdots, n$ and $j = 1, 2, \cdots, q$) represents the translational displacement of the mass component of the jth TMD in the ith TMD group. x_T^i denotes the antinode location of the mode shape of the ith dominant mode with $0 < x_T^n \leqslant x_T^{n-1} \leqslant \cdots \leqslant x_T^1 = l$, thus the location of the ith TMD group. δ is the Dirac delta function [31]. Both subsystems are interconnected through the translational velocity $w_t(x_T^i, t)$ of the SCOLE beam at $x = x_T^i$ and the force generated by the ith TMD group.

In order to simulate the dynamics of the infinite-dimensional SCOLE-TMD model Σ (2.5)-(2.11) and to optimize the TMDs, we use finite element method (FEM) to spatially discretize Σ to a finite-dimensional model Σ_d. The first step is to approximate the solution using a set of high-order basis functions as below

$$w(x,t) = \sum_{k=1}^{N} W_k(t) u_k(x), \tag{2.12}$$

where $u_k(x)$ ($k = 1, 2, \dots N$) is the basis function, which satisfies the essential boundary conditions (2.7), i.e.,

$$u_k(x=0) = \frac{\mathrm{d}u_k}{\mathrm{d}x}(x=0) = 0. \tag{2.13}$$

We denote the coefficients of (2.12) by the vector

$$\mathbf{W} = \begin{bmatrix} W_1 & W_2 & \cdots & W_N \end{bmatrix}^T, \tag{2.14}$$

where the superscript T denotes the nonconjugate transpose. A convenient choice for $u_k(x)$ is the Hermite interpolating polynomials [32], which have been successfully applied to the discretization of the Euler-Bernoulli beam and the Timoshenko beam [33].

Assuming there are $(P+1)$ collocation points along the beam $0 = x_0 < x_1 < \cdots < x_P = l$, we can derive $N = 2P$ piecewise cubic Hermite polynomials u_k satisfying

$$u_{2r-1}(x_c) = \begin{cases} 1, r = c \\ 0, r \neq c \end{cases}, (u_{2r-1})_x(x_c) = 0, \tag{2.15}$$

$$(u_{2r})_x(x_c) = \begin{cases} 1, r = c \\ 0, r \neq c \end{cases}, u_{2r}(x_c) = 0, \tag{2.16}$$

where $r = 1, 2, \cdots, P$ and $c = 0, 1, \cdots, P$. We employ the MATLAB function *pwch* to produce polynomials u_k which are continuous and have compact supports satisfying the property of the function f in (2.13). It is obvious that in (2.14), we have

$$W_{2r-1} = w(x_r, t), W_{2r} = w_x(x_r, t). \tag{2.17}$$

We use the standard Galerkin approach [34] to calculate the weak form of (2.5). After some simple algebra, we derive N equations of motion as

$$\mathbf{M}_p \ddot{\mathbf{W}} + \mathbf{C}_p \dot{\mathbf{W}} + \mathbf{K}_p \mathbf{W} + \mathbf{K}_d \mathbf{h} + \mathbf{C}_d \dot{\mathbf{p}} = \mathbf{E}_F F_e + \mathbf{E}_T T_e, \tag{2.18}$$

where

$$\mathbf{h} = \begin{bmatrix} h^{11} & h^{12} & \cdots & h^{1q} & \cdots & h^{n1} & h^{n2} & \cdots & h^{nq} \end{bmatrix}^T, \tag{2.19}$$

$$\mathbf{p} = \begin{bmatrix} p^{11} & p^{12} & \cdots & p^{1q} & \cdots & p^{n1} & p^{n2} & \cdots & p^{nq} \end{bmatrix}^T, \tag{2.20}$$

in which

$$h^{ij}(t) = p^{ij}(t) - w(x_T^i, t). \tag{2.21}$$

The coefficient matrices in (2.18) are

$$\mathbf{M}_p = \left[m\mathbf{u}_m\mathbf{u}_m^T + J(\mathbf{u}_m)_x(\mathbf{u}_m)_x^T\right]_{x=l} + \int_0^l \rho\mathbf{u}_m\mathbf{u}_m^T \mathrm{d}x \tag{2.22}$$

$$\mathbf{C}_p = q\sum_{i=1}^{n} d_i\mathbf{u}_m(x_T^i)\mathbf{u}_m(x_T^i)^T \tag{2.23}$$

$$\mathbf{K}_p = \int_0^l EI(\mathbf{u}_m)_{xx}(\mathbf{u}_m)_{xx}^T \mathrm{dx} \tag{2.24}$$

$$\mathbf{K}_d(:,b) = -k_i\mathbf{u}_m(x_T^i) \tag{2.25}$$

$$\mathbf{C}_d(:,b) = -d_i\mathbf{u}_m(x_T^i) \tag{2.26}$$

$$\mathbf{E}_F = \mathbf{u}_m(l) \tag{2.27}$$

$$\mathbf{E}_T = (\mathbf{u}_m)_x(l), \tag{2.28}$$

where $\mathbf{u}_m = \begin{bmatrix} u_1 & u_2 & \cdots & u_N \end{bmatrix}^T$, $b = 1, 2, \ldots N_T$ (recall that N_T is the total number of TMDs) and $i = \lceil (b/q) \rceil$ where $\lceil x \rceil$ denotes the smallest integer not less than x. Besides, the following equations of motion for the TMDs can be easily derived:

$$\begin{aligned} \dot{\mathbf{h}} &= \mathbf{h}_W\dot{\mathbf{W}} + \dot{\mathbf{p}}, & (2.29)\\ \ddot{\mathbf{p}} &= \mathbf{p}_W\dot{\mathbf{W}} + \mathbf{K}_T\mathbf{h} + \mathbf{C}_T\dot{\mathbf{p}}, & (2.30) \end{aligned}$$

where

$$\begin{aligned} \mathbf{h}_W(b,:) &= -\mathbf{u}_m(x_T^i)^T, & (2.31)\\ \mathbf{p}_W(b,:) &= \frac{d_i}{m_{ij}}\mathbf{u}_m(x_T^i)^T, & (2.32)\\ \mathbf{K}_T(b,b) &= -\frac{k_i}{m_{ij}}, & (2.33)\\ \mathbf{C}_T(b,b) &= -\frac{d_i}{m_{ij}}. & (2.34) \end{aligned}$$

Here $i = \lceil (b/q) \rceil$ and $j = b - (i-1)q$. $\mathbf{K}_T$ and $\mathbf{C}_T$ are diagonal matrices.

Now we get the state space formulation of the spatially discretized SCOLE-TMD model Σ_d from (2.18), (2.29) and (2.30):

$$\begin{cases} \dot{\mathbf{X}} = \mathbf{A}\mathbf{X} + \mathbf{B}\mathbf{u} & (2.35)\\ \mathbf{Y} = \mathbf{C}\mathbf{X}, & (2.36) \end{cases}$$

where the state $\mathbf{X} = \begin{bmatrix} \mathbf{W} & \dot{\mathbf{W}} & \mathbf{h} & \dot{\mathbf{p}} \end{bmatrix}^T$ and the input $\mathbf{u} = [F_e, T_e]^T$. The system matrix $\mathbf{A}$ and the input matrix $\mathbf{B}$ are

$$\mathbf{A} = \begin{bmatrix} \mathbf{0} & \mathbf{I} & \mathbf{0} & \mathbf{0} \\ -\mathbf{M}_p^{-1}\mathbf{K}_p & -\mathbf{M}_p^{-1}\mathbf{C}_p & -\mathbf{M}_p^{-1}\mathbf{K}_d & -\mathbf{M}_p^{-1}\mathbf{C}_d \\ \mathbf{0} & \mathbf{h}_W & \mathbf{0} & \mathbf{I} \\ \mathbf{0} & \mathbf{p}_W & \mathbf{K}_T & \mathbf{C}_T \end{bmatrix},$$

$$\mathbf{B} = \begin{bmatrix} \mathbf{0} & \mathbf{0} \\ \mathbf{M}_p^{-1}\mathbf{E}_F & \mathbf{M}_p^{-1}\mathbf{E}_T \\ \mathbf{0} & \mathbf{0} \\ \mathbf{0} & \mathbf{0} \end{bmatrix}, \tag{2.37}$$

where $\mathbf{I}$ is the identity matrix. Note that $\mathbf{A} \in \mathbb{R}^{n_d \times n_d}$, $\mathbf{B} \in \mathbb{R}^{n_d \times 2}$ and $n_d = 2N + 2N_T$. If $\mathbf{Y} = \begin{bmatrix} w(x_1,t) & w(x_2,t) & \cdots & w(x_P,t) \end{bmatrix}^T$ (beam displacements at the collocation points), we get the output

matrix $\mathbf{C} = [\mathbf{T}\ \mathbf{0}\ \mathbf{0}\ \mathbf{0}]$ where $\mathbf{T}(r, 2r-1) = 1$ and $\mathbf{T} \in \mathbb{R}^{P\times N}$. If $\mathbf{Y} = [w(x_T^1, t)\ w(x_T^2, t)\ \cdots w(x_T^n, t)]^T$ (beam displacements at the locations of TMD groups), we have

$$\mathbf{C} = \left[\mathbf{C}_W\ \mathbf{0}\ \mathbf{0}\ \mathbf{0}\right], \tag{2.38}$$

$$\mathbf{C}_W(i,:) = \mathbf{u}_m(x_T^i)^T, \mathbf{C}_W \in \mathbb{R}^{n\times N}. \tag{2.39}$$

The transfer function matrix of Σ_d is

$$\mathbf{H}(s) = \mathbf{C}\left(s\mathbf{I} - \mathbf{A}\right)^{-1}\mathbf{B}. \tag{2.40}$$

Based on Σ_d, we are not only able to conduct the optimal TMDs' design using the $\mathcal{H}_\infty$ and $\mathcal{H}_2$ optimizations, but also able to simulate the dynamics of the SCOLE beam system (for example using the MATLAB built-in function *lsim*).

III. Optimization of TMDs for Vibration Suppression of the Non-Uniform SCOLE model

In this section, we employ the $\mathcal{H}_\infty$ and $\mathcal{H}_2$ optimizations to derive the parameters of the multiple TMDs in the spatially discretized SCOLE-TMD model Σ_d (2.35) - (2.36) to achieve optimal vibration reduction. For the system under harmonic excitations, it is desirable to develop a control mechanism to minimize the peak magnitude of the system frequency response, which is associated with $\mathcal{H}_\infty$ optimization. If the system is subject to random excitations, it is more appropriate to take the RMS value of the system response as the performance index for optimization design, which is linked with the system's $\mathcal{H}_2$ optimization [35], [36]. In terms of vibration control, some frequencies are of particular interest since the excitations in real world usually have limited frequency bands and mainly affect narrow bands around dominant modal frequencies of the systems with little or no damping. Therefore, we utilize the frequency-limited versions of $\mathcal{H}_\infty$- and $\mathcal{H}_2$-norms [37], [38] in the optimization of TMD parameters, i.e., computing the $\mathcal{H}_\infty$- and $\mathcal{H}_2$-norms over bounded frequency intervals around dominant modal frequencies of the SCOLE model, which is numerically cheaper. Note that the modal frequencies of the SCOLE model are absolute values of the imaginary parts of the eigenvalues of $\mathbf{A}$ in Σ_d (2.35) - (2.36) excluding TMDs. We can derive the mode shapes by pre-multiplying eigenvectors of $\mathbf{A}$ by $\mathbf{T}_v = \left[\mathbf{T}\quad \mathbf{0}\right] \in \mathbb{R}^{P\times 2N}$.

We consider the external force and torque $\left[F_e\quad T_e\right]^T$ as excitations (inputs) and beam displacements at the locations of TMD groups $\left[w(x_T^1,t)\quad w(x_T^2,t)\quad \cdots\quad w(x_T^n,t)\right]^T$ (i.e., antinode positions of the mode shapes of the dominant modes) as outputs. We use $\|\mathbf{H}\|_{\infty,\left[\omega_l^i,\omega_r^i\right]}$ and $\|\mathbf{H}\|_{2,\left[\omega_l^i,\omega_r^i\right]}$ to denote the frequency-limited $\mathcal{H}_\infty$- and $\mathcal{H}_2$-norms of the transfer function matrix $\mathbf{H}$ (2.40) of Σ_d (2.35) - (2.36) over the frequency range $[\omega_l^i, \omega_r^i]$ (in rad/s, $\omega_l^i, \omega_r^i \in \mathbb{R}^+$, $\omega_l^i < \omega_r^i$) around the ith dominant modal frequency ω_i, respectively. The numerical computation of $\|\mathbf{H}\|_{2,\left[\omega_l^i,\omega_r^i\right]}$ was based on the Gramian-based formulation [38].

We now introduce our optimization scheme, starting with the simple case of n TMD groups with each group having a single TMD (i.e., $q = 1$). They are tuned to suppress the n dominant modes of the SCOLE model. If the control purpose is only to improve effectiveness of TMDs without considering robustness against mistuning effects, the objective functions to minimize the response of the SCOLE-TMD system Σ_d under harmonic and random excitations are

$$f_{hc}(\mathbf{x}) = \max(\|\mathbf{H}\|_{\infty,\left[\omega_l^1,\omega_r^1\right]}, \|\mathbf{H}\|_{\infty,\left[\omega_l^2,\omega_r^2\right]}, \cdots, \|\mathbf{H}\|_{\infty,\left[\omega_l^n,\omega_r^n\right]}), \tag{3.41}$$

$$f_{rc}(\mathbf{x}) = \sqrt{\textstyle\sum_{i=1}^n \|\mathbf{H}\|_{2,\left[\omega_l^i,\omega_r^i\right]}^2}, \tag{3.42}$$

respectively. Here $\mathbf{x}$ is the vector of design variables with

$$\mathbf{x} = \left[\mathbf{m}_T\ \boldsymbol{\omega}_T\ \boldsymbol{\zeta}\right]^T, \tag{3.43}$$

among which

$$\begin{aligned} \mathbf{m}_T &= \left[m_T^1\ m_T^2\ \cdots\ m_T^n\right], \\ \boldsymbol{\omega}_T &= \left[\omega_T^1\ \omega_T^2\ \cdots\ \omega_T^n\right], \\ \boldsymbol{\zeta} &= \left[\zeta_1\ \zeta_2\ \cdots\ \zeta_n\right], \end{aligned} \tag{3.44}$$

whose elements have been explained after equation (2.4).

If we only consider the robustness of TMDs against mistuning effects under harmonic excitations, the objective function is defined as

$$f_h(\mathbf{x}) = f_{hc}(\mathbf{x}_s) + f_{hc}(\mathbf{x}) + f_{hc}(\mathbf{x}_b), \tag{3.45}$$

where

$$\mathbf{x}_s = \begin{bmatrix} \mathbf{I} & \mathbf{0} & \mathbf{0} \\ \mathbf{0} & 0.9\mathbf{I} & \mathbf{0} \\ \mathbf{0} & \mathbf{0} & \mathbf{I} \end{bmatrix} \mathbf{x}, \tag{3.46}$$

$$\mathbf{x}_b = \begin{bmatrix} \mathbf{I} & \mathbf{0} & \mathbf{0} \\ \mathbf{0} & 1.1\mathbf{I} & \mathbf{0} \\ \mathbf{0} & \mathbf{0} & \mathbf{I} \end{bmatrix} \mathbf{x}, \tag{3.47}$$

and $\mathbf{I}$ is the identity matrix of size n. This means that in (3.45) we take into account $\pm 10\%$ deviations of the central frequencies of all TMD groups to include mistuning effects for robust control design. Similarly, for random excitations, the robustness objective function is

$$f_r(\mathbf{x}) = f_{rc}(\mathbf{x}_s) + f_{rc}(\mathbf{x}) + f_{rc}(\mathbf{x}_b). \tag{3.48}$$

In view of the trade-off between effectiveness and robustness, we respectively enforce the following constraints for (3.45) and (3.48)

$$f_{hc}(\mathbf{x}) \leq \theta_h, , \tag{3.49}$$

$$f_{rc}(\mathbf{x}) \leq \theta_r, . \tag{3.50}$$

In (3.49), the value of θ_h can be selected between $f_{hc}(\mathbf{x}_e^*)$ and $f_{hc}(\mathbf{x}_r^*)$ where $\mathbf{x}_e^*$ and $\mathbf{x}_r^*$ are the minimizers of objective functions (3.41) (which only considers effectiveness) and (3.45) (which only considers robustness), respectively. As we increase the value of θ_h, the effectiveness of the TMD system decreases while its robustness against mistuning effects grows, and vice versa. The value of θ_r in (3.50) is set using the same idea. For optimization of the TMD system with each TMD group having multiple TMDs ($q > 1$) to control a dominant mode, we add a design variable $\mathbf{B}_W = \left[B_W^1\ B_W^2\ \cdots\ B_W^n\right]$ in addition to those in the vector (3.43), which contains the non-dimensional frequency bandwidths of the n TMD groups as shown in (2.1). The optimization mechanism is the same as the case of $q = 1$, thus omitted.

We use the MATLAB sequential quadratic programming (SQP) algorithm *fmincon* as a tool to derive the optimal parameters of the TMD system. In practice, the ratio between the total mass of the TMD system and the mass of the main structure is usually chosen between 1% and 2% [13], [14]. During our optimization procedure, we set it as a constant. Besides, to ensure stability of the finite-dimensional SCOLE-TMD model Σ_d (2.35) - (2.36), the real parts of all the eigenvalues of the system matrix $\mathbf{A}$ are constrained to be negative.

IV. Simulation Study

In this section we test our optimization scheme proposed in Section III against the traditional methods for the TMD design through simulation studies on the SCOLE-TMD model under harmonic and random excitations. The model has following properties: $l = 1$ m, $\rho(x)$ =0.2 kg/m - 0.1 (kg/m^2) x, $EI(x)$ =0.2 N·m^2 - 0.1 N·m x, $m = 0.05$ kg and $J = 0.1$ kg·m^2. The total mass of the SCOLE beam system is therefore 0.2 kg. The collocation points are uniformly distributed along the beam: $x_r = rh$, $r = 1, 2, \cdots, P$, where

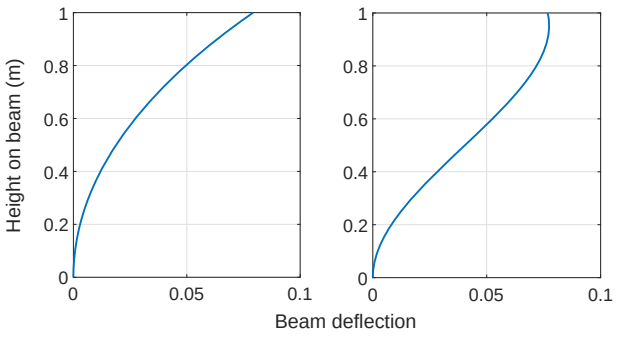

Fig. 3. Mode shapes of the first two modes of the SCOLE model. The left-hand diagram shows the mode shape of the first mode while the right-hand one is the mode shape of the second mode.

$h = l/P$. Without loss of generality, we assume the torque excitation T_e is very small and negligible, and regard the force F_e as the only excitation source.

The modal mass M_i for the ith mode of the SCOLE model is

$$M_i = \frac{\left[\int_0^l \rho(x) Y_i(x) \mathrm{d}x + m Y_i(l)\right]^2}{\int_0^l \rho(x) Y_i^2(x) \mathrm{d}x + m Y_i^2(l)}, \tag{4.51}$$

where $Y_i(x)$ denotes the mode shape of the ith mode. According to the description at the beginning of Section III, we derive the first two modal frequencies

$$\omega_1 = 1.1203\,\text{rad/s} \quad \text{and} \quad \omega_2 = 4.6184\,\text{rad/s} \tag{4.52}$$

with their corresponding mode shapes in Fig. 3. The antinode of the first mode shape is located at $x = 1\,\text{m}$ (the beam top) while the antinode of the second mode shape is at $x = 0.95\,\text{m}$. The modal masses for the first two modes are

$$M_1 = 0.08095\,\text{kg} \quad \text{and} \quad M_2 = 0.09988\,\text{kg}, \tag{4.53}$$

respectively. In total they make up 90.41% of the mass of the SCOLE beam, which implies that the first two modes play dominant roles in the dynamic response of the SCOLE beam. Hence, we only take them into account for vibration control. We devise two TMD groups at locations $x_T^1 = 1\,\text{m}$ and $x_T^2 = 0.95\,\text{m}$. The frequency interval $[\omega_l^i, \omega_r^i]$ $(i = 1,\ 2)$ around each modal frequency ω_i for frequency-limited $\mathcal{H}_\infty$ and $\mathcal{H}_2$ optimizations is chosen to be $[0.7\omega_i, 1.3\omega_i]$. We mention that we only talk about the simulation results at $x = 1\,\text{m}$ while the conclusion on results at $x = 0.95\,\text{m}$ are similar, thus omitted.

We choose the number of collocation points $P = 10$ in the optimization of TMD parameters and dynamic simulation of the SCOLE-TMD model. Ideally, the value of P should be independent of $\mathcal{H}_\infty$- and $\mathcal{H}_2$-norms, which implies that as P increases, the $\mathcal{H}_\infty$- and $\mathcal{H}_2$-norms of the SCOLE-TMD system should converge within a small range. $P = 10$ satisfies this rule with a relative error of the order of 10^{-4} for both norms when P is chosen from $7, 8, \cdots, 13$.

A. Simulation Studies under Harmonic Excitations

In this section, we design various TMD systems for the case of the SCOLE beam subject to harmonic excitations using Den Hartog's formulae [4] and our scheme proposed in Section III respectively, and compare their performances. For the TMD system with $q = 1$ (each TMD group has a single TMD) we first determine the optimal parameters of TMDs by Den Hartog's formulae which are

$$\frac{(\omega_T^i)^2}{\omega_i^2} = \frac{1}{(1+\mu_i)^2}, \tag{4.54}$$

$$\zeta_i = \sqrt{\frac{3\mu_i}{8(1+\mu_i)}}, \tag{4.55}$$

where $i = 1, 2$. ω_T^i and ζ_i are the optimal central frequency and the optimal average damping ratio of the ith TMD group, respectively. ω_i is the ith modal frequency of the SCOLE beam. $\mu_i = \frac{m_T^i}{M_i}$ is the mass ratio of the ith TMD group where m_T^i and M_i are the total mass of the ith TMD group and the modal mass of the ith mode as in (4.51), respectively. μ_i should be specified according to the realistic situation. All the other parameters of the TMD system can be obtained through equations (2.1)–(2.4). We set $\mu_1 = \mu_2 = 0.02$, which means that the total mass of each TMD group is 2% of the corresponding modal mass. Together with the values of ω_i and M_i from (4.52) and (4.53), we get the TMD system T_D using the above Den Hartog's formulae, whose parameters are listed in Table I. The total mass of the TMD system is 0.003617 kg. We use the same total mass for TMDs in our frequency-limited $\mathcal{H}_\infty$ optimizations under harmonic excitations, which derive all other TMD systems in Table I. Table I also lists the values of objective functions f_{hc} (3.41) and f_h (3.45) for these optimal TMD systems, and the values of the constraint θ_h in (3.49) for the trade-off between effectiveness and robustness of some TMD systems.

In Table I, T_{hs}^1–T_{hs}^4 have a single TMD in each of the two TMD groups (i.e, $q = 1$). First we design T_{hs}^1 and T_{hs}^4 by only considering effectiveness with the objective function (3.41) and by only considering robustness against mistuning effects with the objective function (3.45), respectively. Then we design T_{hs}^2 and T_{hs}^3 by taking into account the trade-off between effectiveness and robustness with the objective function (3.45) and the constraint (3.49) through changing the value of θ_h in (3.49) in a range between the lower bound 35.67 m/N (the value of the effectiveness objective function (3.41) f_{hc}^* for T_{hs}^1) and the upper bound 60.26 m/N (the value of (3.41) f_{hc}^* for T_{hs}^4). T_{hm}^1–T_{hm}^4 have 11 TMDs in each of the two TMD groups (i.e., $q = 11$). They are designed similarly as the case that each TMD group has a single TMD. Please refer the caption of Table I for further information contained in the notation of each TMD system.

Fig. 4 shows the displacement root-mean-square (RMS) of the SCOLE model at $x = 1$ m, stabilized by T_D, T_{hs}^1 and T_{hm}^1 of Table I respectively, under harmonic excitations

$$F_e = 0.0001 \text{ N } sin(\omega_e t), \tag{4.56}$$

where the excitation frequency ω_e ranges from $0.8\omega_1$ to $1.2\omega_1$ and from $0.8\omega_2$ to $1.2\omega_2$. In Fig. 4, T_{hs}^1 optimized by our method reduces the peak displacement RMS by 61.34% from the case with T_D designed using Den Hartog's formulae, which demonstrates that our optimization scheme achieves a better performance than Den Hartog's formulae. Recall that, in both cases, a single TMD is tuned for each dominant mode. Besides, T_{hm}^1 reduces the peak displacement RMS by 17.93% from the case with T_{hs}^1, which shows that the TMD system with each TMD group having multiple TMDs to suppress a dominant mode is more effective than the TMD system with each TMD group having a single TMD. The improved effectiveness achieved by T_{hs}^1 over T_D and by T_{hm}^1 over T_{hs}^1 agree with Table I, where the value of the effectiveness objective function f_{hc}^* (the smaller, the more effective) drops by 67.15% from T_D to T_{hs}^1 and by 20.51% from T_{hs}^1 to T_{hm}^1.

The trade-off between effectiveness and robustness is evaluated through mistuning by multiplying the flexural rigidity function EI by a coefficient α which is varied between 0.81 and 1.21 so the modal frequencies of the SCOLE beam vary by $\pm 10\%$. Fig. 5 shows the peak displacement RMS of the SCOLE model (for a range of α) stabilized by the TMD systems in Table I. For each α, the peak displacement RMS is the maximal displacement RMS over the excitation frequencies $\left\{\omega_e : \bigcup_{i=1}^2 \omega_e/\omega_i \in [0.8,\, 1.2]\right\}$. Thus, Fig. 5 can be used to assess the robustness of each TMD system against mistuning effects.

Table II lists the maximum of the peak displacement RMS values over α, along with the peak displacement RMS at $\alpha = 1$, for each of the TMD systems in Table I, as well as their percent changes from the case with T_D. We use the peak displacement RMS for the original model (at $\alpha = 1$) in Fig. 5 and Table II to evaluate the effectiveness of each TMD system, where it is clear that effectiveness from T_{hs}^1 to T_{hs}^4 and from T_{hm}^1 to T_{hm}^4 decrease. Such trends are expected from the value of the effectiveness

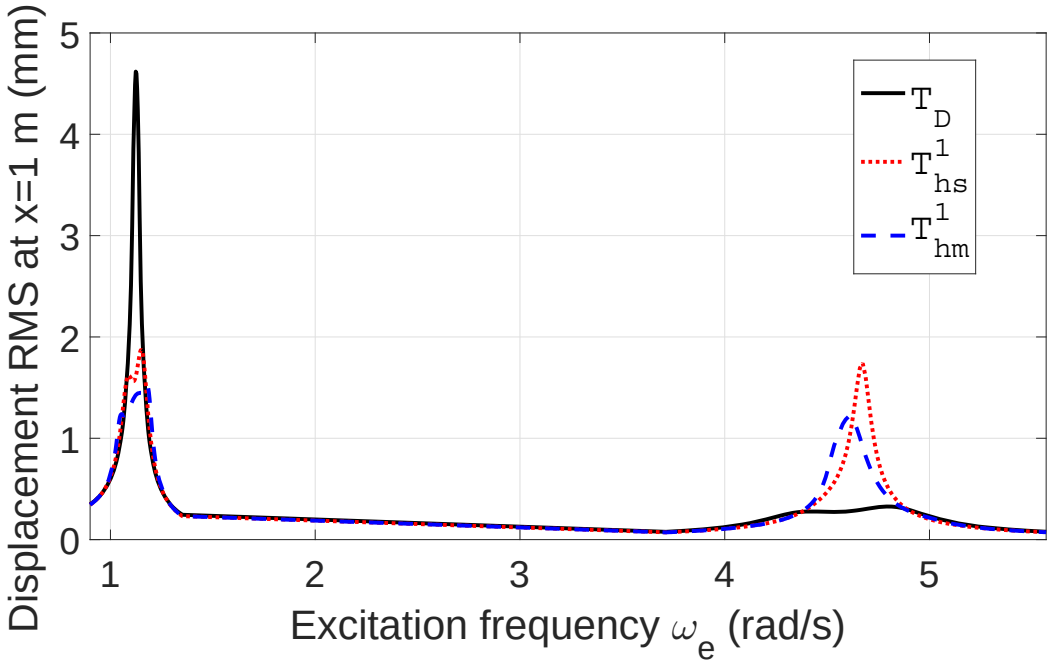

Fig. 4. Beam-top displacement RMS values of the SCOLE model stabilized by T_D, T^1_{hs} and T^1_{hm} in Table I versus the excitation frequency ω_e.

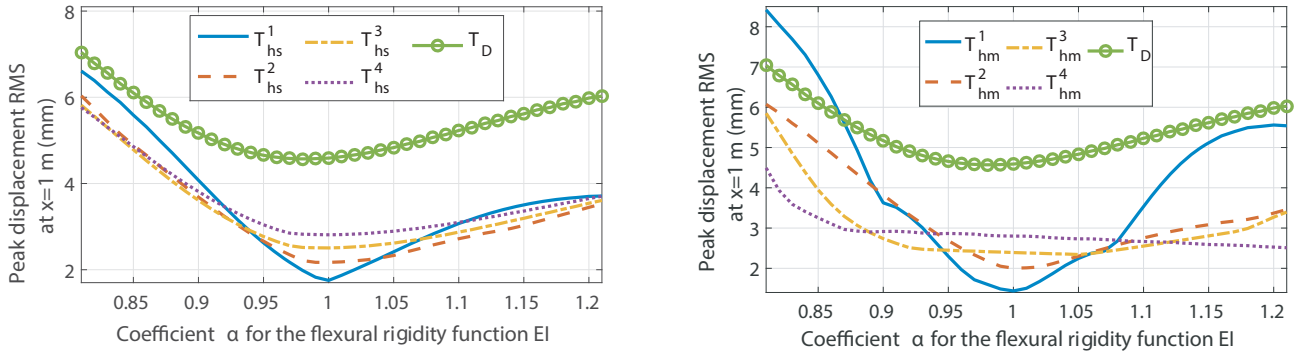

(a) (b)

Fig. 5. Peak beam-top displacement RMS values of the SCOLE model stabilized by the TMD systems in Table I versus the coefficient α for the flexural rigidity function EI under harmonic excitations.

objective function f^*_{hc} (the smaller, the more effective) in Table I. Meanwhile, these TMD systems become increasingly robust with the decreasing of effectiveness as shown in Fig. 5 where the sensitivity of the TMD systems to variations of α reduces, and also as shown in Table II where the maximum of the peak displacement RMS values over α dwindles from T^1_{hs} to T^4_{hs} and from T^1_{hm} to T^4_{hm}. This is expected from the value of the robustness objective function f^*_h (the smaller, the more robust) in Table I.

From Table I, as the constraint θ_h in (3.49) increases, the value of the effectiveness objective function f^*_{hc} increases while the value of the robustness objective function f^*_h decreases. This shows that the trade-off between effectiveness and robustness is achieved by adjusting the value of θ_h in (3.49) when optimizing TMD parameters. Moreover, with a same value of θ_h, TMD systems with $q = 11$ are generally more effective and more robust than those with $q = 1$. T^1_{hm} is the most effective among all the TMD systems for the original model ($\alpha = 1$), but is the least robust against variations of modal frequencies induced by the varying α. Clearly from Fig. 5, except T^1_{hm}, all the other TMD systems optimized by our scheme are

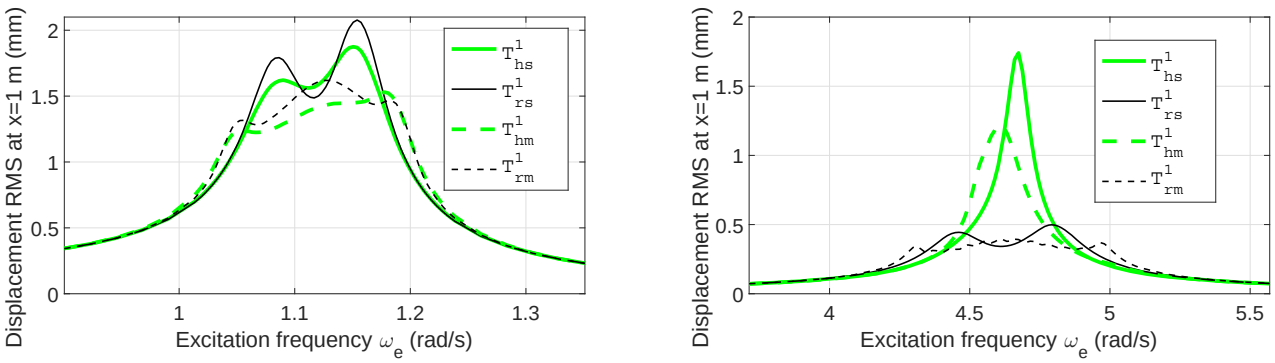

Fig. 6. Beam-top displacement RMS values of the SCOLE model stabilized by T_{hs1} & T_{hm1} in Table I and T_{rs1} & T_{rm1} in Table III versus the excitation frequency ω_e.

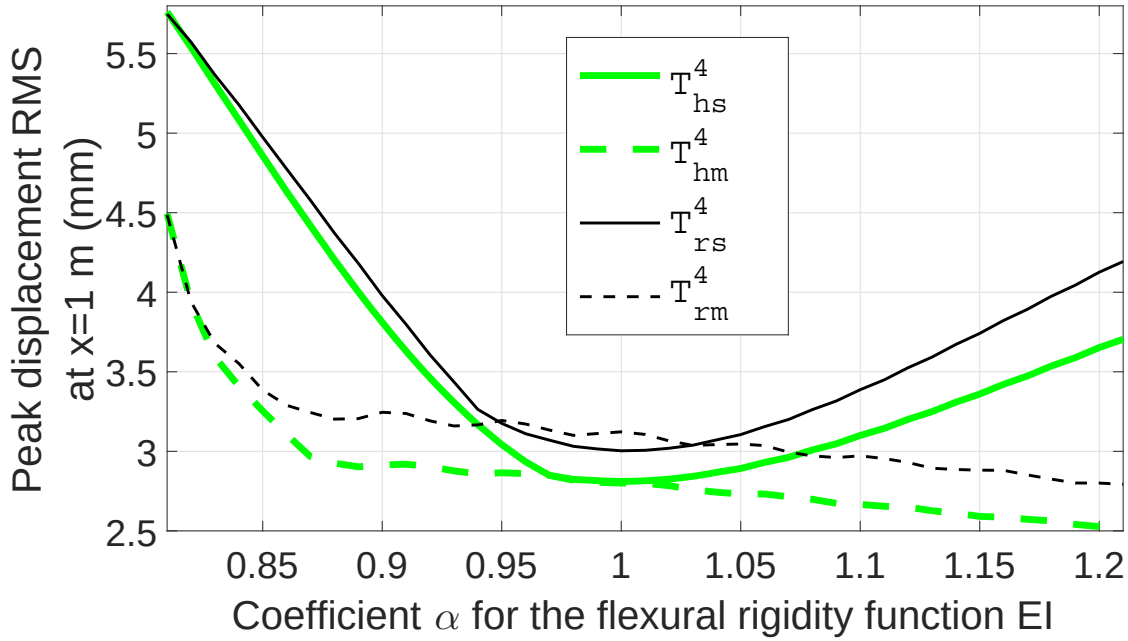

Fig. 7. Peak beam-top displacement RMS values of the SCOLE model stabilized by T_{hs4} & T_{hm4} in Table I and T_{rs4} & T_{rm4} in Table III versus the coefficient α for the flexural rigidity function EI under harmonic excitations.

more effective than T_D derived by Den Hartog's formulae over the whole range of α.

Now we compare the performances of T_{hs1} and T_{hm1} in Table I (designed by $\mathcal{H}_\infty$ optimization) against T_{rs1} and T_{rm1} in Table III (designed by $\mathcal{H}_2$ optimization), as shown in Fig. 6. These 4 TMD systems are designed by only considering effectiveness. As expected, the peak displacement RMS values of the SCOLE model stabilized by TMD systems based on $\mathcal{H}_\infty$ optimization are lower than their counterparts designed by $\mathcal{H}_2$ optimization. In addition, we compare the performances of T_{hs4} and T_{hm4} in Table I (designed by $\mathcal{H}_\infty$ optimization) against T_{rs4} and T_{rm4} in Table III (designed by $\mathcal{H}_2$ optimization). All these four TMD systems are designed by only considering robustness. As shown in Fig. 7, over the range of α, TMD systems designed based on $\mathcal{H}_\infty$ optimization are generally more effective than their counterparts designed by $\mathcal{H}_2$ optimization. These results verify that $\mathcal{H}_\infty$ optimization is more suitable than $\mathcal{H}_2$ optimization for the design of TMD systems to suppress vibrations due to harmonic excitations.

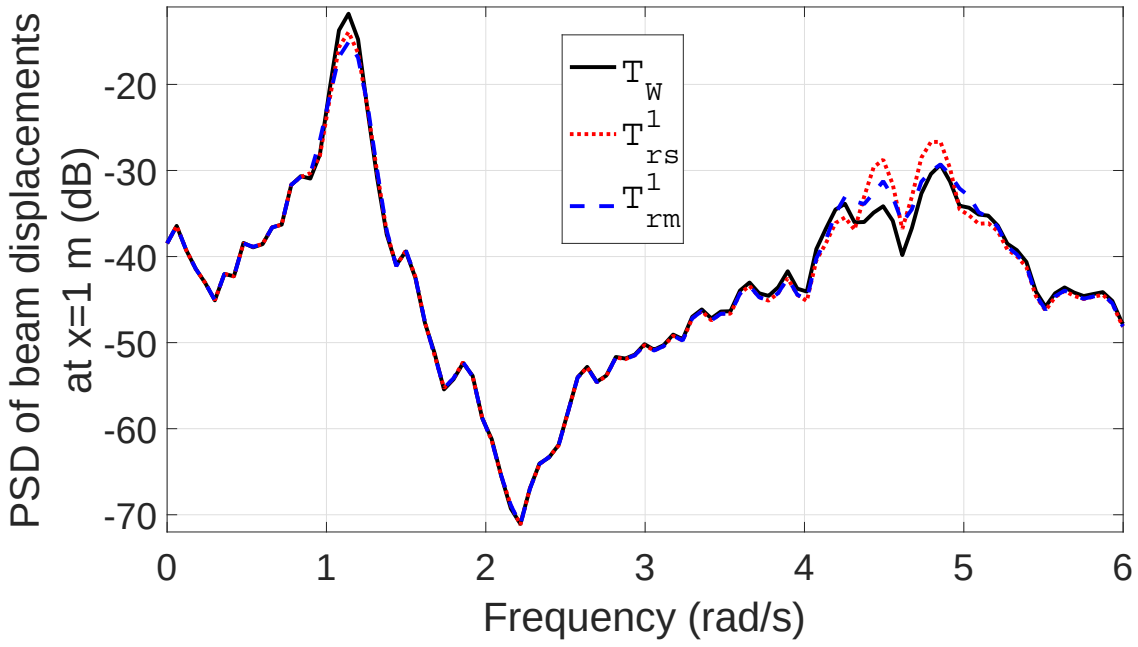

Fig. 8. PSD of beam-top displacements of the SCOLE model stabilized by T_W, T^1_{rs} and T^1_{rm} in Table III.

B. Simulation Studies under Random Excitations

We now design various TMD systems for the case of the SCOLE beam being subject to random excitations using Warburton's formulae [7] and our scheme proposed in Section III respectively, and compare their performances. For the TMD system with $q = 1$ (each TMD group has a single TMD) we first determine the optimal parameters of TMDs by Warburton's formulae which are

$$\frac{(\omega^i_T)^2}{\omega_i^2} = \frac{2+\mu_i}{2(1+\mu_i)^2}, \tag{4.57}$$

$$\zeta_i = \sqrt{\frac{\mu_i(4+3\mu_i)}{8(1+\mu_i)(2+\mu_i)}}. \tag{4.58}$$

Similarly as the case for harmonic excitations, with $\mu_1 = \mu_2 = 0.02$ and the values of ω_i and M_i from (4.52) and (4.53), we get the TMD system T_W using the above Warburton's formulae, whose parameters are listed in Table III. We derive all other TMD systems of Table III using the frequency-limited $\mathcal{H}_2$ optimizations under random excitations. The procedures are similar as those in Section IV-A, thus omitted. All these TMD systems have the same total mass of 0.003617 kg. Table III also lists the values of corresponding objective functions f_{rc} (3.42) and f_r (3.48), and the trade-off constraint θ_r in (3.50) between effectiveness and robustness, during optimization.

Fig. 8 shows the power spectral densities (PSDs) of displacements of the SCOLE model stabilized by TMD systems T_W, T^1_{rs} and T^1_{rm} in Table III (see the caption of Table III for the meaning of the TMD system's notation.), under a random excitation. The excitation $F(t)$ is generated by passing a Gaussian pulse process, with a variance of 0.001 N^2 and sampling time of 0.002 s, through a 10th-order bandpass Butterworth filter whose passband and stopband frequencies are 1 Hz and 1.2 Hz respectively to cover the first and second modal frequencies of the SCOLE model. It is clear from Fig. 8 that TMD system T^1_{rs} optimized by our method has better vibration reduction performances around the first modal frequency than T_W designed using Warburton's formulae, but is not as good as T_W around the second modal frequency. However, the later result shown in Fig. 9a validates that the overall effectiveness of T^1_{rs} is better than T_W.

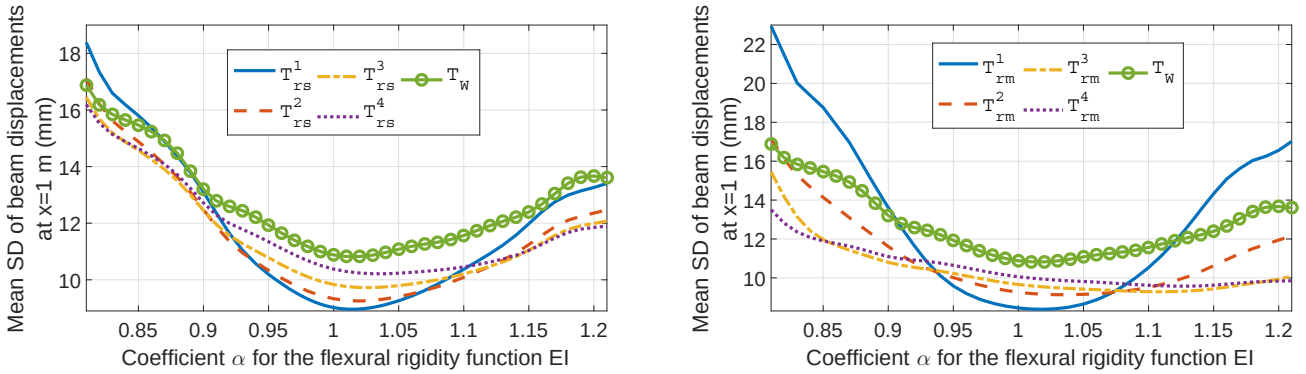

(a) (b)

Fig. 9. Mean SDs of beam-top displacements of the SCOLE model stabilized by the TMD systems in Table III versus the coefficient α for the flexural rigidity function EI under random excitations.

In addition, performances of T^1_{rm} are slightly better than T^1_{rs} around both modal frequencies. These agree with Table III, where the value of the effectiveness objective function f^*_{rc} (the smaller, the more effective) drops by 21.39% from T_W to T^1_{rs} and drops by 6.58% from T^1_{rs} to T^1_{rm}. We conclude that our optimization scheme achieves better performance than Warburton's formulae and that the TMD system with each TMD group having multiple TMDs to suppress a dominant mode is more effective than the TMD system with each TMD group having a single TMD.

Like Section IV-A, we introduce a varied coefficient α for the flexural rigidity function EI to evaluate the trade-off between effectiveness and robustness. 50 different realizations of the excitation characterized above are generated using 50 different random seeds. For the SCOLE model at a certain value of α stabilized by each TMD system, the standard deviation (SD) of beam-top displacements is computed for each excitation; these 50 SDs are then averaged to form a mean SD. Fig. 9 shows these mean SDs for the TMD systems in Table III as functions of the coefficient α, which can be used to assess the robustness of these TMD systems against mistuning effects. Table IV lists the maximum of the mean SDs over α, along with the mean SD at $\alpha = 1$, for each of the TMD systems in Table III, as well as their percent changes from the case with T_W. Table III, Fig. 9 and Table IV have similar trends as Table I, Fig. 5 and Table II of Section IV-A. According to Table III, the trade-off between effectiveness and robustness can be made by adjusting the value of θ_r in the constraint (3.50) when optimizing TMD parameters. T^1_{rm} is the most effective among all the TMD systems for the original model ($\alpha = 1$), but is the least robust against mistuning effects. From Fig. 9, except T^1_{rm}, the TMD systems optimized by our scheme are more effective than T_W derived by Warburton's formulae over most of the range of α considered.

Similarly as the end of Section IV-A, we compare performances of TMD systems in Table I (designed by $\mathcal{H}_\infty$ optimization) against the ones in Table III (designed by $\mathcal{H}_2$ optimization) subject to random excitations. The mean SD of displacements of the SCOLE model (at $\alpha = 1$) with T_{hs1} (T_{hm1}) is 14.64% (15.09%) larger than the case with T_{rs1} (T_{rm1}). From these results, along with Fig. 10, we verify that $\mathcal{H}_2$ optimization is more suitable for the design of optimal TMD systems for the SCOLE model subject to random excitations than $\mathcal{H}_\infty$ optimization.

V. Conclusions

In this paper, we have proposed a method for the design of optimal TMD systems to suppress the vibrations of flexible structures described by PDEs. We took the non-uniform SCOLE model as an illustrative application. We used multiple groups of TMDs with each group placed at the antinode of the mode shape of a dominant mode of the SCOLE model. Then we employed finite element method to discretize this infinite-dimensional SCOLE-TMD model to be a finite-dimensional model Σ_d which was

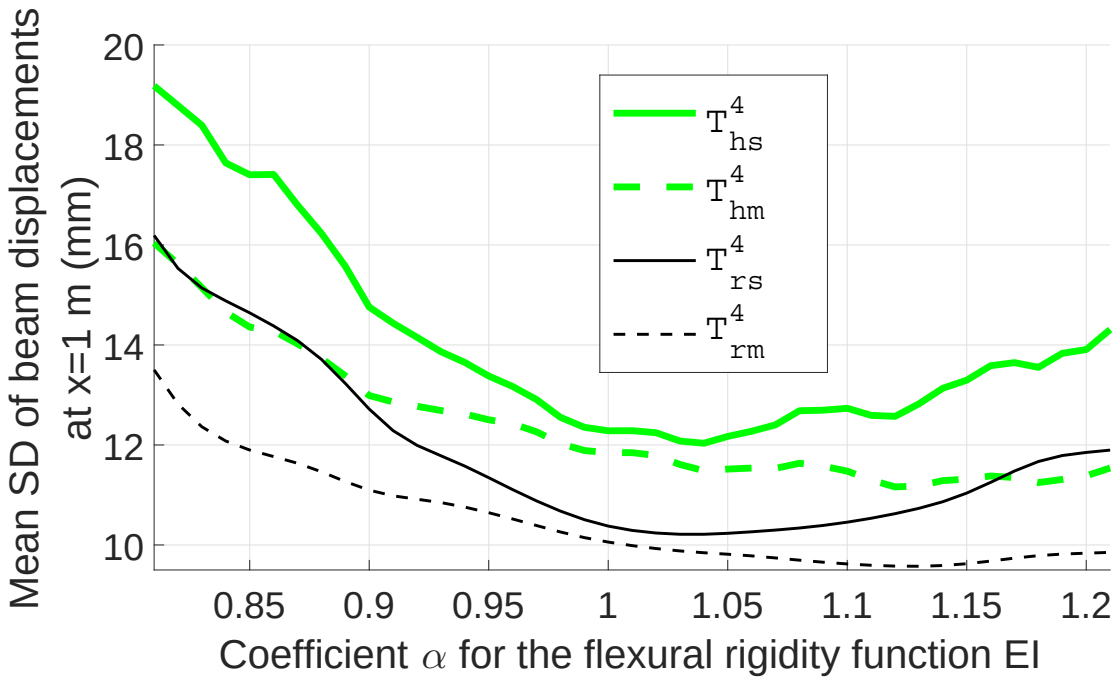

Fig. 10. Mean SDs of beam-top displacements of the SCOLE model stabilized by T_{rs}^4 & T_{rm}^4 in Table III and T_{hs}^4 & T_{hm}^4 in Table I versus the coefficient α for the flexural rigidity function EI under random excitations.

used for control design based on frequency-limited versions of $\mathcal{H}_\infty$ and $\mathcal{H}_2$ optimizations. TMD systems derived by our scheme are able to suppress multiple dominant vibration modes simultaneously.

Our simulation tests showed that the performances of the TMD systems with a single TMD tuned for each dominant mode designed by our methods are superior to the ones derived by traditional methods (Den Hartog's formulae and Warburton's formulae). In addition our methods can specify the trade-off between effectiveness and robustness. We demonstrated that the TMD systems with multiple TMDs tuned for each dominant mode are more effective and robust than the TMD systems with a single TMD tuned for each dominant mode.

REFERENCES

[1] F. Sadek, B. Mohraz, A. W. Taylor, and R. M. Chung, "A method of estimating the parameters of tuned mass dampers for seismic applications," *Earthquake Engineering and Structural Dynamics*, vol. 26, pp. 617–635, 1997.

[2] Date of access: 21/02/2017. [Online]. Available: http://www.amusingplanet.com/2014/08/the-728-ton-tuned-mass-damper-of-taipei.html

[3] J. J. Connor, *Introduction to Structural Motion Control*. Upper Saddle River, New Jersey: Prentice Hall Pearson Education, 2003.

[4] J. P. D. Hartog, *Mechanical Vibration*, 4th ed. New York: McGraw-Hill Book Company, 1956.

[5] P. H. Wirsching and G. C. Campbell, "Minimal structural response under random excitation using the vibration absorber," *Earthquake Engineering and Structural Dynamics*, vol. 2, no. 4, pp. 303–312, 1974.

[6] R. J. McNamara, "Tuned mass dampers for buildings," *Journal of the Structural Division*, vol. 103, no. 9, pp. 1785–1798, 1977.

[7] G. B. Warburton, "Optimum absorber parameters for various combinations of response and excitation parameters," *Earthquake Engineering and Structural Dynamics*, vol. 10, no. 3, pp. 381–401, 1982.

[8] D. Younesian, E. Esmailzadeh, and R. Sedaghati, "Passive vibration control of beams subjected to random excitations with peaked PSD," *Journal of Vibration and Control*, vol. 12, no. 9, pp. 941–953, 2006.

[9] A. Y. T. Leung, H. Zhang, C. C. Cheng, and Y. Y. Lee, "Particle swarm optimization of TMD by non-stationary base excitation during earthquake," *Earthquake Engineering and Structural Dynamics*, vol. 37, pp. 1223–1246, 2008.

[10] K. Xu and T. Igusa, "Dynamic characteristics of multiple substructures with closely spaced frequencies," *Earthquake Engineering and Structural Dynamics*, vol. 21, pp. 1059–1070, 1992.

[11] H. Yamaguchi, "Fundamental characteristics of multiple tuned mass dampers for suppressing harmonically forced oscillations," *Earthquake Engineering and Structural Dynamics*, vol. 22, pp. 51–62, 1993.

[12] M. Abé and Y. Fujino, "Dynamic characterization of multiple tuned mass dampers and some design formulas," *Earthquake Engineering and Structural Dynamics*, vol. 23, pp. 813–835, 1994.

[13] T. Igusa and K. Xu, "Vibration control using multiple tuned mass dampers," *Journal of Sound and Vibration*, vol. 175, no. 4, pp. 491–503, 1994.

[14] M. Luu, V. Zabel, and C. Könke, "An optimization method of multi-resonant response of high-speed train bridges using TMDs," *Finite Elements in Analysis and Design*, vol. 53, pp. 13–23, 2012.

[15] A. Kareem and S. Kline, "Performance of multiple mass dampers under random loading," *Journal of Structural Engineering*, vol. 121, no. 2, pp. 348–361, 1995.

[16] A. J. Clark, "Multiple passive tuned mass dampers for reducing earthquake induced building motion," in *9th World Conference on Earthquake Engineering*, Tokyo-Kyoto, Japan, August 1988.

[17] L. Bergman, D. McFarland, J. Hall, E. Johnson, and A. Kareem, "Optimal distribution of tuned mass dampers in wind-sensitive structures," in *Proceedings of ICOSSAR 89, the 5th International Conference on Structural Safety and Reliability, Part I*, San Francisco, USA, August 1989, pp. 95–102.

[18] R. Lewandowski and J. Grzymisawska, "Dynamic analysis of structures with multiple tuned mass dampers," *Journal of Civil Engineering and Management*, vol. 15, no. 1, pp. 77–86, 2009.

[19] K. S. Moon, "Vertically distributed multiple tuned mass dampers in tall buildings: performance analysis and preliminary design," *The Structural Design of Tall and Special Buildings*, vol. 19, no. 3, pp. 347–366, 2010.

[20] T. S. Fu and E. A. Johnson, "Distributed mass damper system for integrating structural and environmental controls in buildings," *Journal of Engineering Mechanics*, vol. 137, no. 3, pp. 205–213, 2011.

[21] B. Z. Guo, "On boundary control of a hybrid system with variable coefficients," *Journal of Optimization Theory and Applications*, vol. 114, pp. 373–395, 2002.

[22] W. Littman and L. Markus, "Stabilization of a hybrid system of elasticity by feedback boundary damping," *Annali di Matematica Pura ed Applicata*, vol. 152, no. 1, pp. 281–330, 1988.

[23] ——, "Exact boundary controllability of a hybrid system of elasticity," *Archive for Rational Mechanics and Analysis*, vol. 103, pp. 193–235, 1988.

[24] X. Zhao and G. Weiss, "Suppression of the vibrations of wind turbine towers," *IMA Journal of Mathematical Control and Information*, vol. 28, pp. 377–389, 2011.

[25] X. Tong, X. Zhao, and S. Zhao, "Load reduction of a monopile wind turbine tower using optimal tuned mass dampers," *International Journal of Control*, vol. 90, no. 7, pp. 1283–1298, 2017.

[26] J. Jonkman, S. Butterfield, W. Musial, and G. Scott, "Definition of a 5-MW reference wind turbine for offshore system development," National Renewable Energy Laboratory, CO, USA, Tech. Rep. NREL/TP-500-38060, 2009.

[27] J. M. Jonkman and M. L. Buhl Jr, "FAST user's guide," National Renewable Energy Laboratory, CO, USA, Tech. Rep. NREL/EL-500-38230, 2005.

[28] T. Fitzpatrick, P. Dallard, S. L. Bourva, A. Low, R. R. Smith, and M. Willford, *Linking London: The Millennium Bridge*. London: The Royal Academy of Engineering, 2001.

[29] C. C. Lin, J. F. Wang, and B. L. Chen, "Train-induced vibration control of high-speed railway bridges equipped with multiple tuned mass dampers," *Journal of Bridge Engineering*, vol. 10, no. 4, pp. 398–414, 2005.

[30] M. Abé and T. Igusa, "Tuned mass dampers for structures with closely spaced natural frequencies," *Earthquake Engineering and Structural Dynamics*, vol. 243, pp. 247–261, 1995.

[31] S. Hassani, "Dirac delta function," in *Mathematical methods for students of physics and related fields*, 2nd ed. New York: Springer, 2009, pp. 139–170.

[32] I. H. Shames and C. L. Dym, *Energy and finite element methods in structural mechanics*. New York: Taylor & Francis, 1985.

[33] G. Falsone and D. Sattineri, "An Euler-Bernoulli-like finite element method for Timoshenko beams," *Mechanics Research Communications*, vol. 38, no. 1, pp. 12–16, 2011.

[34] T. R. Chandrupatla and A. D. Belegundu, *Introduction to finite elements in engineering*, 3rd ed. Upper Saddle River, New Jersey: Prentice Hall Pearson Education, 2002.

[35] L. Zuo and S. Nayfeh, "Design of passive mechanical systems via decentralized control techniques," in *43rd AIAA/ASME/ASCE/AHS/ASC Structures, Structural Dynamics, and Materials Conference*, Denver, USA, April 2002.

[36] L. Zuo, "Effective and robust vibration control using series multiple tuned-mass dampers," *Journal of Vibration and Acoustics*, vol. 131, no. 3, p. 031003, 2009.

[37] R. Toscano, "Signal and system norms," in *Structured Controllers for Uncertain Systems*, 1st ed. London: Springer, 2013, pp. 25–44.

[38] P. Vuillemin, C. Poussot-Vassal, and D. Alazard, "Poles residues descent algorithm for optimal frequency-limited $\mathcal{H}_2$ model approximation," in *2014 European Control Conference*, Strasbourg, France, June 2014, pp. 1080–1085.

TABLE I

THE OPTIMAL PARAMETERS OF 9 TMD SYSTEMS AND THE VALUES OF CORRESPONDING OBJECTIVE FUNCTIONS f_{hc} (3.41) AND f_h (3.45) AT THESE OPTIMAL PARAMETERS (ALL DENOTED BY SUPERSCRIPT $*$) FOR THE SCOLE-TMD SYSTEM UNDER HARMONIC EXCITATIONS. q IS THE NUMBER OF TMDS IN EACH TMD GROUP. θ_h IN CONSTRAINT (3.49) IS SET FOR THE TRADE-OFF BETWEEN EFFECTIVENESS AND ROBUSTNESS. IN THE NOTATION OF TMD SYSTEMS, THE SUBSCRIPT D (OR h) MEANS THAT THE TMD SYSTEM IS DESIGNED BY DEN HARTOG'S FORMULAE (OR $\mathcal{H}_\infty$ OPTIMIZATION) TO SUPPRESS HARMONIC EXCITATIONS; THE SUBSCRIPT s (OR m) MEANS THAT EACH TMD GROUP HAS A SINGLE (OR MULTIPLE) TMDS; THE SUPERSCRIPT 1-4 IS THE TMD SYSTEM'S INDEX (WITH ITS INCREASING, A TMD SYSTEM'S EFFECTIVENESS DECREASES AND ROBUSTNESS INCREASES).

TMD system	q	m_T^{1*} (g)	m_T^{2*} (g)	ω_T^{1*} (rad/s)	ω_T^{2*} (rad/s)	ζ_1^*	ζ_2^*	B_W^{1*}	B_W^{2*}	θ_h (m/N)	f_{hc}^* (m/N)	f_h^* (m/N)
T_D	1	1.619	1.998	1.098	4.528	0.08575	0.08575	-	-	-	108.6	608.5
T_{hs}^1	1	3.415	0.202	1.112	4.528	0.04880	0.04268	-	-	-	35.67	419.3
T_{hs}^2	1	3.466	0.151	1.112	4.637	0.06453	0.04887	-	-	40	40.00	355.9
T_{hs}^3	1	3.467	0.150	1.108	4.625	0.08074	0.06531	-	-	50	50.00	332.7
T_{hs}^4	1	3.483	0.134	1.103	4.628	0.09748	0.07287	-	-	-	60.26	326.4
T_{hm}^1	11	3.420	0.197	1.115	4.773	0.01275	0.009135	0.1113	0.09364	-	28.32	1301
T_{hm}^2	11	3.460	0.157	1.112	4.640	0.06412	0.03936	0.01324	0.07917	40	40.00	357.1
T_{hm}^3	11	3.380	0.237	1.123	4.460	0.02826	0.08340	0.1882	0.004000	50	50.00	309.4
T_{hm}^4	11	3.341	0.276	1.141	4.725	0.01608	0.07034	0.2538	0.2424	-	61.77	202.4

TABLE II

MAXIMUM OF THE PEAK BEAM-TOP DISPLACEMENT RMS VALUES OVER α (THE COEFFICIENT FOR THE FLEXURAL RIGIDITY FUNCTION EI), ALONG WITH THE PEAK BEAM-TOP DISPLACEMENT RMS AT $\alpha = 1$, FOR EACH OF THE TMD SYSTEMS IN TABLE I, AS WELL AS THEIR PERCENT CHANGES FROM THE CASE WITH T_D. IN THE NOTATION OF TMD SYSTEMS, THE SUBSCRIPT D (OR h) MEANS THAT THE TMD SYSTEM IS DESIGNED BY DEN HARTOG'S FORMULAE (OR $\mathcal{H}_\infty$ OPTIMIZATION) TO SUPPRESS HARMONIC EXCITATIONS; THE SUBSCRIPT s (OR m) MEANS THAT EACH TMD GROUP HAS A SINGLE (OR MULTIPLE) TMDS; THE SUPERSCRIPT 1-4 IS THE TMD SYSTEM'S INDEX (WITH ITS INCREASING, A TMD SYSTEM'S EFFECTIVENESS DECREASES AND ROBUSTNESS INCREASES).

TMD system	Maximum of the peak displacement RMS values over α (mm)	Percent change	Peak displacement RMS at $\alpha = 1$ (mm)	Percent change
T_D	7.041	-	4.622	-
T_{hs}^1	6.609	-6.137%	1.871	-59.52%
T_{hs}^2	6.034	-14.30%	2.182	-52.79%
T_{hs}^3	5.815	-17.41%	2.513	-45.63%
T_{hs}^4	5.762	-18.16%	2.815	-39.10%
T_{hm}^1	8.419	19.57%	1.504	-67.46%
T_{hm}^2	6.074	-13.74%	2.012	-56.47%
T_{hm}^3	5.851	-16.90%	2.382	-48.46%
T_{hm}^4	4.494	-36.18%	2.799	-39.45%

TABLE III

THE OPTIMAL PARAMETERS OF 9 TMD SYSTEMS AND THE VALUES OF CORRESPONDING OBJECTIVE FUNCTIONS f_{rc} (3.42) AND f_r (3.48) AT THESE OPTIMAL PARAMETERS (ALL DENOTED BY SUPERSCRIPT $*$) FOR THE SCOLE-TMD SYSTEM UNDER RANDOM EXCITATIONS. q IS THE NUMBER OF TMDS IN EACH TMD GROUP. θ_r IN CONSTRAINT (3.50) IS SET FOR THE TRADE-OFF BETWEEN EFFECTIVENESS AND ROBUSTNESS. IN THE NOTATION OF TMD SYSTEMS, THE SUBSCRIPT W (OR r) MEANS THAT THE TMD SYSTEM IS DESIGNED BY WARBURTON'S FORMULAE (OR $\mathcal{H}_2$ OPTIMIZATION) TO SUPPRESS HARMONIC EXCITATIONS; THE SUBSCRIPT s (OR m) MEANS THAT EACH TMD GROUP HAS A SINGLE (OR MULTIPLE) TMDS; THE SUPERSCRIPT 1-4 IS THE TMD SYSTEM'S INDEX (WITH ITS INCREASING, A TMD SYSTEM'S EFFECTIVENESS DECREASES AND ROBUSTNESS INCREASES).

TMD system	q	m_T^{1*} (g)	m_T^{2*} (g)	ω_T^{1*} (rad/s)	ω_T^{2*} (rad/s)	ζ_1^*	ζ_2^*	B_W^{1*}	B_W^{2*}	θ_r (m/N)	f_{rc}^* (m/N)	f_r^* (m/N)
T_W	1	1.619	1.998	1.104	4.550	0.07019	0.07019	-	-	-	11.25	46.84
T_{rs}^1	1	2.783	0.834	1.114	4.600	0.03637	0.04422	-	-	-	8.844	46.34
T_{rs}^2	1	2.820	0.797	1.112	4.596	0.05480	0.06379	-	-	9.2	9.200	41.74
T_{rs}^3	1	2.815	0.802	1.111	4.592	0.07078	0.08590	-	-	9.8	9.800	40.26
T_{rs}^4	1	2.794	0.823	1.111	4.593	0.08514	0.1140	-	-	-	10.44	39.93
T_{rm}^1	11	2.804	0.813	1.119	4.636	0.006741	0.008196	0.1123	0.1302	-	8.262	77.36
T_{rm}^2	11	2.849	0.768	1.121	4.613	0.03319	0.04817	0.1409	0.08988	9.2	9.200	41.27
T_{rm}^3	11	2.846	0.771	1.131	4.672	0.01190	0.01414	0.2197	0.2220	9.8	9.800	35.11
T_{rm}^4	11	2.846	0.771	1.135	4.693	0.01137	0.01257	0.2493	0.2586	-	10.34	33.20

TABLE IV

MAXIMUM OF THE MEAN SDS OF BEAM-TOP DISPLACEMENTS OVER α (THE COEFFICIENT FOR THE FLEXURAL RIGIDITY FUNCTION EI), ALONG WITH THE MEAN SD AT $\alpha = 1$, FOR EACH OF THE TMD SYSTEMS IN TABLE III, AS WELL AS THEIR PERCENT CHANGES FROM THE CASE WITH T_W. IN THE NOTATION OF TMD SYSTEMS, THE SUBSCRIPT W (OR r) MEANS THAT THE TMD SYSTEM IS DESIGNED BY WARBURTON'S FORMULAE (OR $\mathcal{H}_2$ OPTIMIZATION) TO SUPPRESS HARMONIC EXCITATIONS; THE SUBSCRIPT s (OR m) MEANS THAT EACH TMD GROUP HAS A SINGLE (OR MULTIPLE) TMDS; THE SUPERSCRIPT 1-4 IS THE TMD SYSTEM'S INDEX (WITH ITS INCREASING, A TMD SYSTEM'S EFFECTIVENESS DECREASES AND ROBUSTNESS INCREASES).

TMD system	Maximum of the mean SDs of displacements over α (mm)	Percent change	Mean SD of displacements at $\alpha = 1$ (mm)	Percent change
T_W	16.87	-	10.82	-
T_{rs}^1	18.38	8.974%	8.964	-17.16%
T_{rs}^2	17.11	1.438%	9.268	-14.34%
T_{rs}^3	16.45	-2.501%	9.761	-9.787%
T_{rs}^4	16.19	-4.029%	10.29	-4.888%
T_{rm}^1	22.95	36.02%	8.399	-22.37%
T_{rm}^2	17.18	1.829%	9.193	-15.03%
T_{rm}^3	15.45	-8.402%	9.588	-11.39%
T_{rm}^4	13.50	-19.96%	9.987	-7.698%